Vol. 17(9), pp. 202-211, September 2023
DOI: 10.5897/AJMR2023.9698
Article Number: 873D54A71167
ISSN: 1996-0808

http://www.academicjournals.org/AJMR

ACADEMIC JOURNALS
expand your knowledge

African Journal of Microbiology Research

Full Length Research Paper

Effect of methylprednisolone on the morphology of acute lymphoblastic leukemia cell line *in vitro* model by Atomic Force Microscopy

Amairani Moreno-Caro[1], Edgar Sandoval-Petris[1], Josue Juarez[2], Miguel A. Valdez[2], Leonardo Ibor Ruiz-Ortega[4], Homero Rendón-García[3] and María G. Burboa-Zazueta[1]*

[1]Departamento de Investigaciones Científicas y Tecnológicas de la Universidad de Sonora, C.P. 83000, Hermosillo, Sonora México.
[2]Departamento de Física, Universidad de Sonora, C. P. 83000, Hermosillo, Sonora, México.
[3]Hospital Infantil del Estado del Sonora, Reforma 355, C. P. 83100 Hermosillo, Sonora, México.
[4]Department of Biological Sciences, Columbia University, New York, NY, 10027, USA.

Received 4 April, 2023; Accepted 24 August, 2023

Despite the recent knowledge of the molecular mechanisms of corticosteroid drugs in lymphoid leukemia, information about the nanostructured surface morphology of the process of cell death is limited. Therefore, the main objective of this work is to analyze the effect of methylprednisolone on the morphology of B lymphoblast CCRF-SB cell line by Atomic Force Microscopy (AFM). Morphological parameters such as height, cell diameter, and roughness were analyzed and used as indicator of cell surface damage. In accordance with AFM images, CCRF-SB cells show an ovoid shape, with a nucleus which occupies a great area of the cytoplasm delimited by the cellular membrane. When a CCRF-SB cells cell was exposed to the drug, the morphology of the cell changed. After 24 h, CCRF-SB cells remains in its ovoid shape; however, AFM images show irregularities that indicate disruption of the cellular membrane and the formation of cellular bodies in the cytoplasm and nucleus. Interestingly, AFM images showed dramatically changes in the morphology of the CCRF-SB cell after 48 h, where fragmentation of the cytoplasm and nucleus were recorded, as result of the cellular death process. These changes in the cellular morphology of CCRF-SB cell can be associated with the cell damage and death process caused by drugs such as methylprednisolone and can be used to control their effectiveness and to establish a correct diagnosis in cancer treatment.

Key words: Glucocorticoids, atomic force microscopy (AFM), cancer cells, CCRF-SB cell, roughness, nuclear cell fragmentation.

INTRODUCTION

Cancer was the cause of nearly 10 million deaths in 2020 in the world, which is nearly one in six of all deaths. The most common types of cancer in 2020 were: Breast (2.26 million), Lung (2.21 million), Colon (1.93 million), among

*Corrresponding author. E-mail: maria.burboa@unison.mx. Tel: +1 52 6621116567.

others (Chhikara and Parang, 2023).

Leukemia is the cancer of blood including white blood cells. There are different types of leukemia: acute lymphoblastic leukemia (ALL), acute myeloid leukemia (AML), and chronic lymphocytic leukemia (CLL); they all affect different age groups. Approximately 474,519 new cases of leukemia contributing 2.5% of total cancer appeared in 2020. Even when leukemia deaths were about 3.1% of all cancer deaths in 2020, leukemia is the most frequent cause of cancer death in children and persons younger than 39 years old (Chhikara and Parang, 2023). Of all leukemias, ALL has the major incidence (about 76%) with the highest rate in children less than 1 year old. Since time ago, leukemia treatments are based on chemotherapy with anthracyclines (Chhikara and Parang, 2010; Terwilliger and Abdul-Hay, 2017). Recently, there have been also important developments in drug delivery through nanotechnology formulations (Mayer et al., 2019) and new genetic technologies (Padmakumar et al., 2021).

Glucocorticoids are steroid hormones (Timmermans et al., 2019) used as anti-inflammatory and antineoplastic drugs, especially in hematologic malignancies.

The actions of glucocorticoids have been associated not only to their differentiation-inducing and apoptosis-inducing effects, but also to the modification of several steps of the hematopoietic and/or immune pathway and these have been reported (Yetgin and Özsoylu, 2007). Specifically, the activity of corticoids on lymphoid cells is described in three steps: initiation (the activation of corticosteroid on lymphocytes), decision step (degradation of pro-survival transcription factors, induction of apoptosis by caspase-3 activation, DNA fragmentation, among others), and the execution step (caspases and endonucleases are activated) (Distelhorst, 2002). Besides, it has been found that glucocorticoids are linked with other cellular mechanisms, such as the proteasomal inhibition, concentration changes of Ca, Na, and K ions (Greenstein et al., 2002; Smith and Cidlowski, 2010; Lambrou et al., 2012; Abdoul-Azize et al., 2017). Recent investigations of the effect of glucocorticoids on colitis and other types of cancer reported that their the rapeutical effectiveness remains questionable and suggested future research (Zhang et al., 2020; Mayayo-Peralta et al., 2021). In the case of ALL, Velentza et al. (2021) suggested the use of glucocorticoids to treat this disease, but not for long-term treatments, because of the children's bone health, among other collateral effects.

Methylprednisolone (MP) is one of the most utilized glucocorticoids drugs in the treatment of ALL (McNeer and Nachman, 2010). ALL is one oncological entity, which activates abnormal mechanisms of proliferation, maturation, and differentiation of lymphoid cells, leading to an increase of immature cells (blast) in the blood stream (Conter et al., 2004). ALL has a higher frequency in children population and is one of the most common leukemia reported (Larios-Farak et al., 2016). The most common treatment for ALL, as mentioned earllier, is the chemotherapy that is based on three steps: induction to the remission, consolidation, and maintenance (Kato and Manabe, 2018). Before the first step, steroids like methylprednisolone are supplied for 7 days, to classify the patients in groups, according to a good, regular, or bad response to the treatment (Tissing et al., 2003; Rendón-García et al., 2017).

Usually, the effects of MP have been investigated on the morphology of leukemia cells. These analyses have been restricted only to optical and electronic microscopy techniques (Hiçsönmez et al., 1996; Hiçsönmez et al., 1999; Özbek et al., 1999). However, it is important to investigate the effect of this drug on leukemia cells by analyzing the topographic characteristics (ultrastructure, diameter, height, roughness) with the intention of gaining a better understanding of the mechanisms of action of corticoids at a nanostructural level.

Atomic Force Microscopy (AFM) is commonly used to observe the surface structure of soft and solid materials (Zhao et al., 2019). It has a very sensitive and sharp probe attached at the edge of a microcantilever, very sensitive to small forces (Figure 1). When the tip is approaching the sample surface, atoms of the tip and the surface interact with a very weak force, but it is enough to perturb the oscillation of the cantilever; then, the position of the probe is detected by an optical sensor, converting this information in a topographical image. From this image, we obtain the relative height of a point to another one and the morphological characteristics from the surface of a given sample (Patel and Kranz, 2018). AFM offers a variety of methods allowing the study of the topography of cells with high resolution (Lastella et al., 2007; Wu et al., 2009; Francis et al., 2010). For instance, AFM was used to analyze the effect of a drug on the cell surface and evaluate the morphological changes in cancer cells with the aim of investigating the morphological changes in the death processes. Through the analysis of the topographic AFM images, it is possible to differentiate a healthy cell from a malignant one by comparing the topographical differences between these cells (Wang et al., 2009; Kim et al., 2012; Pillet et al., 2013; Deng et al., 2018). Specifically, this technique has been used to evaluate roughness and elasticity of cytoskeleton. Therefore, AFM is suitable for measurements to study cellular tissues in pathology (Cai et al., 2010; Jembrek et al., 2018). In the case of leukemia cells, AFM has been used to study the elastic properties of leukemia cancer cell membranes (Rosenbluth et al., 2006). They found that myeloid leukemias are involved in leukocytosis at a higher rate than lymphoid leukemias. A review by Li et al. (2021) shows the different uses of AFM as a tool for analysis of mechanical properties of cells, organelles, and biomolecules.

Thus, the main objective of this work is to measure the effects of MP on the morphology of cells CCRF-SB of

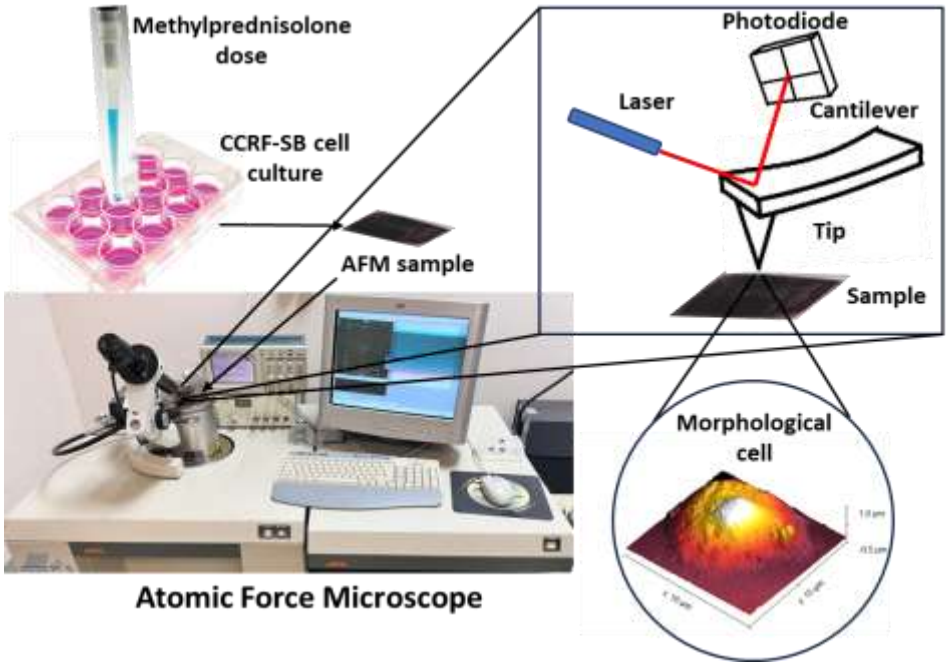

Figure 1. Set-up for an Atomic Force Microscopy. (AFM in the Complex Fluids Lab. University of Sonora)

LLA type B by AFM-based methods and use the parameters such as shape, diameter, height, and roughness to evaluate the cell death process. In general, AFM images show morphological changes such as nuclear and cell fragmentation observed in the cell membrane of CCRF-SB cells, whilst mean roughness (Ra) and mean square roughness (R_q) increased significantly after the drug exposure of 24 and 48 h. In this regard, CCRF-SB cells show an ovoid shape, with a nucleus which occupied a great area of the cytoplasm delimited by the cellular membrane. After 24 h of drug exposition, CCRF-SB cells retained its ovoid shape; however, AFM images show irregularities that indicate disruption of the cellular membrane and the formation of cellular bodies in the cytoplasm and nucleus. After 48 h, interestingly, the morphology of CCRF-SB cells changed and fragmentation of the cytoplasm and nucleus was observed, as a result of the cellular death process. On the other hand, the diameter and height recorded for CCRF-SB cells before the exposition of methylprednisolone were 19 and 0.88 µm, changing to 22 and 1.46 µm, respectively after 24 h of exposition; whilst after 48 h of drug exposition, the diameter and height recorded were 30 and 1.01 µm, respectively.

MATERIALS AND METHODS

Culture cell and methylprednysolone exposition

The B lymphoblast cell line CCRF-SB [CCRF SB] (ATCC ®CCL-120™) was purchased from American Type Culture Collection (ATCC) and used as model of acute lymphoblastic leukemia type B. This cell line has been widely used to investigate ALL, which is the most common type of cancer in childhood (Mendoza-Santiago et al., 2019; Zhao et al., 2020). The CCRF-SB cells were cultured under humidified atmosphere (80-100%) with 5% CO_2 and temperature 37°C. Cells were resuspended in RPMI 1640, supplemented with 10% of bovine fetal serum, amphotericin B 250 µg/ml, penicillin/streptomycin 10,000 IU/ml to 10,000 µg/ml ATCC, gentamycin of 50 mg/ml. Then, CCRF-SB cells were cultured in modified 12-well Petri dishes and exposed to a dose of 845 µM of MP for 24 and 48 h (Özbek et al., 1999).

Sample preparation for AFM analysis

Sterilized supports (mica 1 cm × 1 cm) were used and put in a Petri dish, where 40 µL of L-polylysine (Sigma Aldrich) was added and spread onto the whole surface. After 1 h, the sterilized supports were dried in an incubator. After drying, 50 µl of a CCRF-SB cell suspension (2.5 and 3.0 × 10^4 cells/ml) was added onto the mica surface, incubating for 20 min; after that, cells were fixed with 200 µl formaldehyde (4%) for 5 min.

The use of formaldehyde as a cell fixation agent has been controversial for several years. Szende and Tyihák_ (2010) found that formaldehyde promotes and inhibits the proliferation of cancer cells with different concentrations; Khoirunnisa et al. (2016) have investigated the molecular interaction of formaldehyde and proteins in human cancer cells. On the other hand, the use of formaldehyde as a crosslinking agent is well known (Hoffman et al., 2015) and as fixation agent of cells on solid surfaces, recommending 4% solutions in PBS up to 15 min (Thavarajah et al., 2012). Taking account, the effect of formaldehyde on cells mentioned earlier, we blocked the fixation process of formaldehyde after 5 min. The surface mica was washed three times with PBS (200 µl) and finally, with distilled water to avoid cell damage and the formation of

phosphate crystals during the drying process, prior to AFM observation (Canetta et al., 2014).

Atomic force microscopy

AFM images were recorded with a Jeol JSPM 4210 Japan AFM instrument (Figure 1) with a MikroMasch NSC15/NO AL cantilever with a nominal spring constant of 40 N/m and a resonance frequency around 325 Khz. Images were obtained in the non-contact mode, using a scan size of 70 µm × 70 µm acquired at a scan speed of 3.333 ms^{-1}. These scanning parameters were selected to get a panoramic AFM image with medium quality, in a time of 15 min, and find a CCRF-SB cell. Then after, a manual zoom was carried out on a CCRF-SB cell, and the AFM image was acquired at a scan size of 30 × 30 µm and scan speed of 10.000 ms^{-1}, to get a high-quality topographic image in approximately 45 min.

Surface roughness

The surface roughness (nm) of the samples was analyzed with two parameters: mean roughness (R_a) and mean square roughness (R_q) (Zhao, et al., 2019). R_a is calculated by:

$$R_a = \frac{1}{N_x N_y}\sum_{i=1}^{N_x}\sum_{j=1}^{N_y}\left|Z_{i,j} - Z_{av}\right| \quad , \quad \text{with}$$

$$Z_{av} = \frac{1}{N_x N_y}\sum_{i=1}^{N_x}\sum_{j=1}^{N_y} Z_{i,j} \, , \qquad (1)$$

On the other hand, R_q represents the relative change in the surface roughness of the sample, and it is given by:

$$R_q = \sqrt{\frac{1}{N_x N_y}\sum_{i=1}^{N_x}\sum_{j=1}^{N_y}(Z_{i,j} - Z_{av})^2} \qquad (2)$$

where N_x and N_y are the number of scanning points on the x-axis and y-axis of the AFM image, respectively, $Z_{i,j}$ is the height of the (i,j) point and Z_{av} is the average height of all measuring points from the surface AFM scanning image.

Then, R_a and R_q were determined by randomly sectioning the CCRF-SB cell from the high-quality topographic AFM image (30 × 30 µm) in smaller areas (2 × 2 µm). The cellular sections with artifacts were discarded for roughness analysis.

Data analysis

Software Gwyddion (Nečas and Klapetek, 2012) was used to visualize the morphological parameters of CCRF-SB cells, while quantitative parameters, such as height, diameter, roughness Ra and Rq were determined with the WsxM 5.0 software program (Horcas et al., 2007). The height, diameter, and roughness (Ra and Rq) of CCRF-SB cells were analyzed by one-way nonparametric ANOVA (Kruskal-Wallis) by Minitab Statistical software. This statistical analysis is recommended for small samples, and it is used to determine if there are significant differences between quantitative variables of at least three independent groups. In this case, four AFM images coming from four independent CCRF-SB cells non-exposed and exposed to a dose of MP (845 µM) for 24 and 48 h were analyzed. After nonparametric ANOVA analysis, a post-Hoc test (Tukey) was carried out to determine the statistical significance among data, considering the p values minor to α, the typical significance level (α <0.05).

RESULTS AND DISCUSSION

Ultra structure of CCRF-SB cells

Drugs, viruses, bacteria, etc., can kill a given cell. During the cell death process, the integrity of the cell is damaged modifying its morphological parameters; therefore, in order to understand the death cell process produced by a specific drug, *in vitro* experiments can be conducted to study the cell morphology (Huang et al., 2014).

In this regard, we have investigated the effect of methylprednisolone on the morphology and ultrastructure of CCRF-SB cells, as a B lymphoblast cell model. Lymphoblasts are non-adherent cells, almost always ovoid round shape; these cells are bigger than lymphocytes with a larger cell proportion occupied by the nucleus. It is common to find cells with two nucleoli and cytoplasmic vacuoles.

Figure 2 shows the morphological characteristic of a CCRF-SB cell. It can be observed as a CCRF-SB cell (Figure 2, Image 1) with ovoid round shape, limited by the cell membrane, which result like the shape for health lymphocytes observed by optical microscopy (Laane et al., 2009). Heights of cells are between 1 and 1.5 µ and diameters between 6 and 8 µ. At the nanostructure level (Figure 2, Images 1.1, 1.2, 2.1 and 2.2), we observe components homogeneously distributed along the plasmatic membrane, probably due to the presence of carbohydrates and proteins, which contribute to the structural support of cell membrane (Hu et al., 2009; Huang et al., 2014). Additionally, Figure 2 shows images of CCRF-SB cell in three dimensions (Images 1.3 and 2.3), in which a big nucleus/cytoplasm ratio and protrusions at the edge of the cell membrane can be observed.

Figures 3 and 4 show the AFM images recorded for CCRF-SB cell treated with 845 µM dose of MP after 24 and 48 h, respectively. Changes can be observed in the cell morphology as well as in the ultrastructure of lymphoblasts. Images 3 and 4 in Figure 3 correspond to cells exposed to MP after 24 h. As observed, the morphological changes were small at this time of treatment. On one hand, Images 3.1, 3.2, 4.1 and 4.3 show irregularities on the nucleus of CCRF-SB cell, such gaps (pink arrow in Image 3.1) or pores (Image 4.2). Additionally, in Image 4.3, swelling of cells and invaginations at the edge of the membrane can be observed (yellow arrow, Image 4.3). We note a large increase in cell height, the collapse of the membrane (green arrow, Image 3.3), and the presence of cellular bodies, because of the cellular death process (black arrow in Image 4.3).

The most significant changes in the morphology of

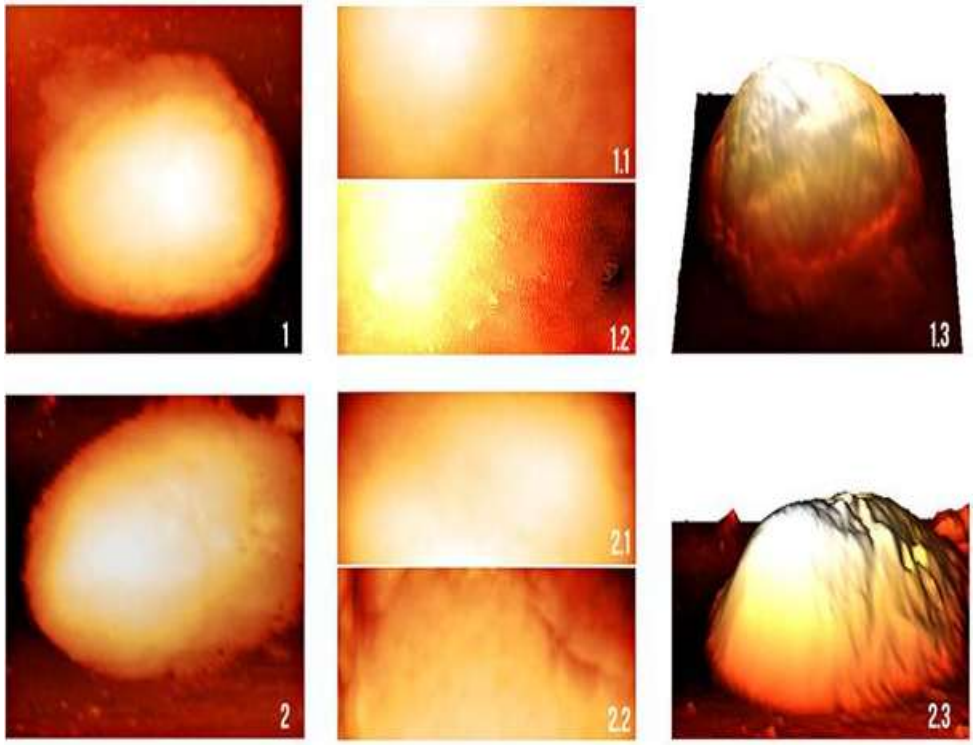

Figure 2. Representative images of the CCRF-SB cell line from a control cell group. Images 1 and 2 correspond to the topographies of the control cells, Images 1.1, 1.2, 2.1, and 2.2 correspond to scanning of 3 × 5 µm and Images 1.3 and 2.3 represents the three-dimensional (3D) cellular structure. Cell 1: Representative control cell, correspond to CCRF-SB without any treatment. 1.1: the ultrastructure of the nucleus, 1.2: ultrastructure of cellular cytoplasm. 1.3: 3D cell morphology. Cell 2: Representative control cell, 2.1: approach in the ultrastructure of the nucleus, 2.2: ultrastructure of cellular cytoplasm and 2.3: 3D morphology of CCRF-SB 2. Images were recorded with a Jeol JSPM 4210 Japan AFM instrument with a nominal spring constant of 40 N/m and a resonance frequency around 325 Khz.

CCRF-SB cell were observed after 48 h in the presence of MP. Some structures can be observed that may be vestiges of cell organelles, even though complementary techniques must be done (White arrow, Figure 4, Image 5.3). The nucleus fragmentation is more evident at the ultrastructure level (Images 6.1 and 6.2); the gap in Image 6.3 showed shrinking of the cell and deep depressions in the membrane cell (red arrow, Image 6.3), such as occurs in the cell necrosis process. Similar effects were also observed in myeloid leukemia cells k-562 exposed to dexamethasone (Wang et al., 2016). Changes on the cellular structure, as well as the formation of cytoplasmatic vacuoles, membane pores, cell shrinkage, protrusions at the edge of the membrane, smooth membrane and irregular nanostructure after the interaction with the drug were also observed. The presence of these damages can result from the apoptotic, necrotic and necroptotic processes (Hu et al., 2009).

On the other hand, we analyzed the morphology of CCRF-SB cell, to understand cellular death processes. Typically, in the cellular death process by apoptosis, the cell shows usual damages like loss of volume, cell shrinkage, apoptotic bodies, and DNA fragmentation. While, in the cell death by necrosis, cytolytic inflammation was observed, loss of membrane integrity, and cellular swelling cause an increase in the cell size. The necroptosis process is a combination of apoptosis and necrosis, both of which demand on a process called autophagy which uses lysosomes to wrap cytoplasm and organelles to make possible cell renewal processes and homeostasis (Walsh and Edinger, 2010). The necroptosis shows different effects on cells; blister-like structures on the cell membranes, cell shrinkage, chromatin condensation and apoptotic bodies formation without membrane rupture. Similarly, drugs of the glucocorticoid's family can activate the apoptosis intrinsic way, as well as the activation of the recruitment mechanism of the ionic channels of Ca^{2+} y Na^{+}, promoting the development of pores on the membrane (Smith and Cidlowski, 2010); therefore, supporting the theory of pores on the membrane, developed by Schwartzman and Cidlowski (1994). They describe the action mechanism of glucocorticoids, which destabilize the plasmatic membrane by a lysis process through pores of

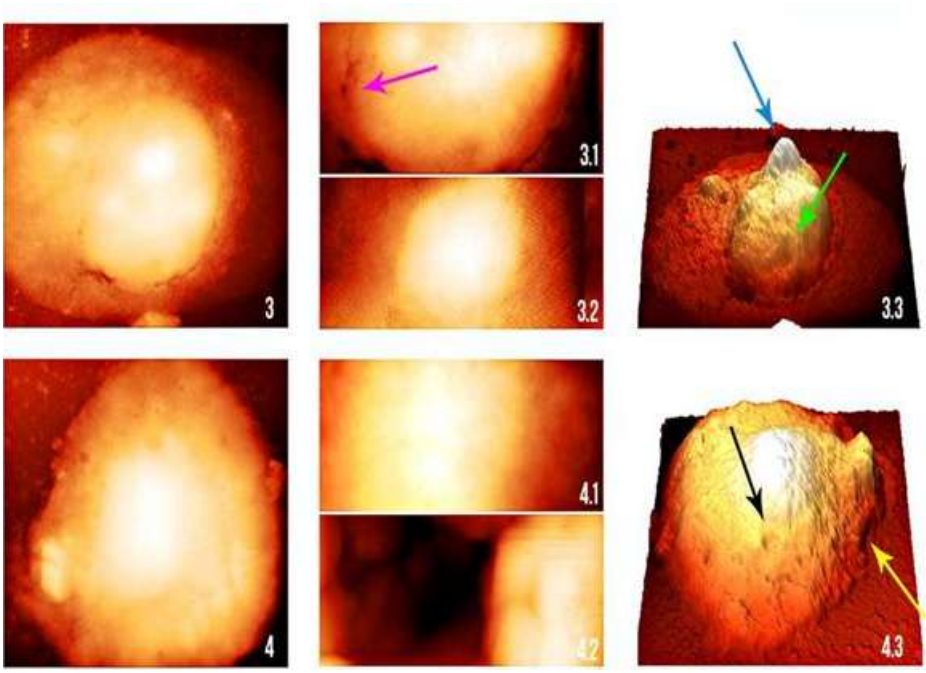

Figure 3. Representative images of the CCRF-SB cell after 24-h exposure with Methylprednisolone. The first column corresponds to the cell topographies, second corresponds to approach of 3 × 5 µm and the third represents the 3D cellular structure. Image 3: Group cell 24 h. Image 3.1: approach in the ultrastructure of the nucleus, pink arrow indicates irregularities in peripheral nuclear membrane, Image 3.2: ultrastructure of cellular cytoplasm. Image 3.3: 3D cell morphology, blue arrow, early nuclear fragmentation, green arrow, nuclear clefts. Image 4: Representative cell of the group 24 h, Image 4.1: approach in the ultrastructure of the nucleus, Image 4.2: cytoplasmic ultrastructure, with special focus on 800 × 800 nm cytoplasmic pore and Image 4.3: 3D morphology of Lymphoblast 4, black arrow, pore location figure 4.2, yellow arrow, early invagination in cytoplasm.

membrane caused by an increase of Ca^{2+} in the cell processes, provoking a concentration difference through the membrane (Pan et al., 2016).

Morphological parameters

Height and diameter

These parameters were analyzed with a non-parametric ANOVA program. The height profile was defined as the difference between the tallest point of cells and the bottom. Results showed non-significant differences between control CCRF-SB cell and cells treated with MP after 24 and 48 h (Table 1). The control cell showed an average height of 0.88 µ and an average diameter of 1.46 µm and 1.01 µm after 24 and 48 h MP of treatment with MP treatment, respectively. Similar results have been reported by Huang et al. (2014), who observed changes in the height of lymphocytes treated with aminophylline for 48 h. These results suggest that the integrity of the cell membrane has been affected due to the MP exposition, affecting the biological characteristic, such as height, diameter, and roughness (Ra and Rq), and eventually, the physiological function of cells (Huang et al., 2014).

Roughness

Roughness is a cytological parameter because it is related with cell processes like cell mechanics, which is also related with adhesion and motility (Antonio et al., 2012); therefore, it is a sensible parameter for the measurement of the state of cells and is intimately bounded with the integrity of the cytoskeleton and the processes that produce structure changes. Then, the change of diameter, height and roughness parameters can be used as a damage sensor in the cell membrane when cells are under cellular death process (apoptosis, necrosis, or necroptosis processes) (Liu et al., 2018).

Roughness values were obtained on random way in section of 2 × 2 µm, neglecting every cell artifact. Figure 5 shows that both Ra and Rq displayed significant differences between non-treated CCRF-SB cells and treated CCRF-SB cells with MP after 24 and 48 h. The

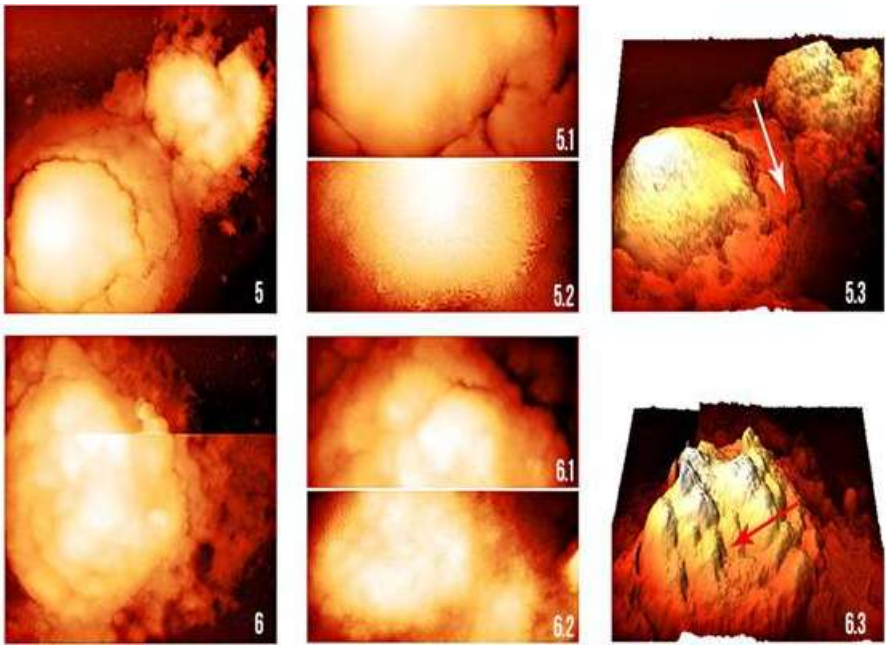

Figure 4. Representative images of CCRF-SB cell with a 48-h exposure time to Methylprednisolone. The first column corresponds to the cellular topographies, the second approach of 3 × 5 µm, and the third representation of the 3D cellular structure. Cell Image 5: Representative cell of the group 48 h. Image 5.1: approach in the ultrastructure of the nucleus, with long fragmentation lines in the peripheries of the nucleus, Image 5.2: ultrastructure of cellular cytoplasm. Image 5.3: 3D cell morphology, white arrow advanced cytoplasmic fragmentation, with cell rupture. Image 6: representative cell of the group 48 h, Image 6.1: approach in the ultrastructure of the nucleus with nuclear fragmentation. Image 6.2: ultrastructure of cytoplasm, and Image 6.3: 3D morphology of Lymphoblast.

Table 1. Cellular size after CCRF-SB cell was exposed to methylprednisolone for 24 and 48 h.

Time of exposition (h)	Diameter (µm) + SD	Height (µm) + SD
0	19 ± 3	0.88 ± 0.07
24	22 ± 6	1.46 ± 0.70
48	30 ± 6	1.01 ± 0.22

Data represent mean of diameter and height. Each group represents the measurements of 4 cells. SD: Standard deviation.

results obtained in this investigation for Ra were 79 ± 15 nm for the control group, 133.4 ± 29.4 nm for cells CCRF-SB with MP exposed 24 h and for cells exposed 48 h was 122.3 ± 16.7 nm. The values of Rq were 93 ± 17, 159.3 ± 34.5, and 141.4 ± 15.4 nm, respectively for the control and the two treatments. These changes in the Ra and Rq values can result from different cellular processes in which the integrity of the cell membrane is compromised. In this regard, Dong et al. (2013) reported changes in the cellular roughness (Ra and Rq) of leukemia lymphoid cells type B exposed to *Staphylococcus aureus*. They observed that the Ra value increased to 3.18 ± 0.35 and 3.07 ± 0.18 nm after the cells were exposed to the Gram (+) bacteria for 24 and 72 h, respectively. While the Rq roughness registered was around 3.93 ± 0.08 and 3.47 ± 0.31 nm, respectively. Dong et al. (2013) explained that the observed changes in Ra and Rq have resulted from the redistribution of the components of the cell membrane that takes place at the surface of the cell (Dong et al., 2013).

Besides the contribution of AFM to the evaluation of changes caused on the morphology and mechanical properties by anticancer drugs on cancer cells, and help to obtain a diagnosis of cancer, there are many other uses of AFM in investigations at molecular level. However, AFM cannot investigate the chemical composition of cells

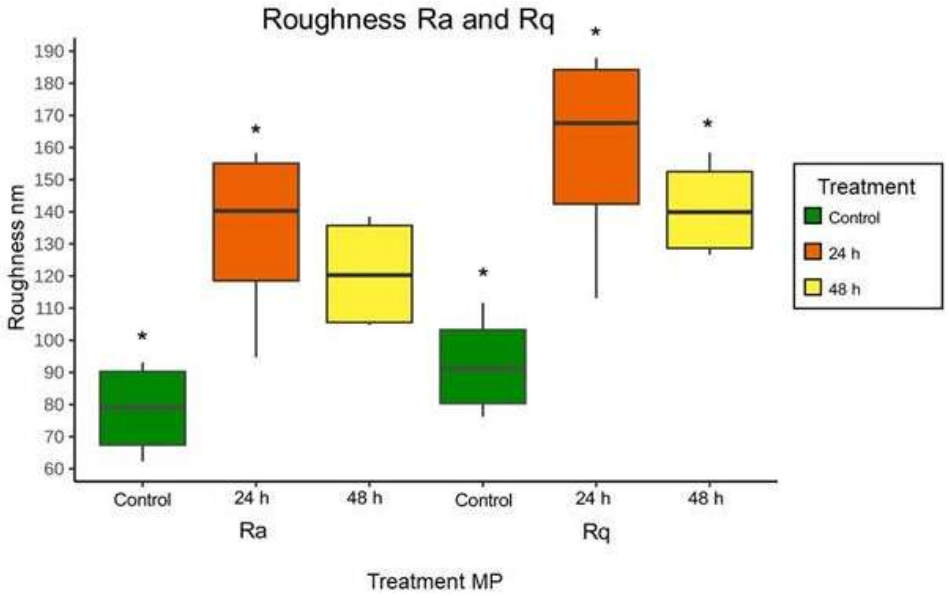

Figure 5. Box plot for cell roughness Ra and Rq subjected to three treatments, control group, treatment with MP at 24 and 48 h. Results represent mean +/- SD of Ra and Rq. Each group represents the measurements in cm/nm/pixel of 4 cells. One-way nonparametric ANOVA (Kluskal-Wallis) followed by Tukey test were used to analyze the Ra and Rq parameters and to compare control cells and cells treated with MP for 24 and 48 h ($p<0.05$).

or molecules and sometimes it is slow to get information on damaged cells, but combined with other techniques like Raman spectroscopy, scanning microscopy confocal laser scanning microscopy, scanning electron microscopy, among others, AFM offers an excellent tool to obtain more precise diagnosis of cancer cells (Deng et al., 2018).

Conclusions

The effects of methylprednisolone (MP) on the morphological properties of leukemia B cell model (CCRF-SB cell line, CCRF-SB) were evaluated by AFM. Before the AFM analysis, a protocol to fix the CCRF-SB CCRF-SB cell onto the mica surface was standardized. It is important to remark that this approach allows to determine the effects of the exposition of MP (845 µM) on the morphology of CCRF-SB cell CCRF-SB by AFM, taking into count parameters such diameter, height, morphology, and roughness. Since these parameters give information about the integrity of the cell membrane, then they have potentials as biomarkers useful to analyze the cellular damages after the exposition of a given drug. In this regard, AFM images allowed to observe the loss of ovoid shape of CCRF-SB cell after cells were exposed to MP for 24 and 48 h. Additionally, despite CCRF-SB retaining its ovoid shape, the exposition to MP for 24 h, topographical irregularities were observed, suggesting that the integrity of the cell membrane has been affected by the exposition to the drug, causing the disruption of the cellular membrane and the formation of cellular bodies in the cytoplasm and nucleus. These effects were more evident after 48 h of exposition to MP, observing fragmentation of the cytoplasm and nucleus of CCRF-SB cells, indicating that cells are dying. These results suggest that the AFM can be considered a powerful tool to study the morphology and topography of cells after the exposition of a given drug. However, AFM tool is limited to be applied in research areas, and it is difficult to be used for clinical purposes due to the time required to prepare the cell sample and to acquire images with high resolution (at least 45 min per image).

CONFLICT OF INTERESTS

The authors have not declared any conflict of interests.

ACKNOWLEDGEMENTS

The authors are grateful to Consejo Nacional de Humanidades, Ciencia y Tecnología (CONAHCYT) for the economic and CONAHCyT (Projects # 2264, 236185, 241133) for the financial support.

REFERENCES

Abdoul-Azize S, Dubus I, Vannier J (2017). Improvement of dexamethasone sensitivity by chelation of intracellular Ca^{2+} in pediatric acute lymphoblastic leukemia cells through the prosurvival kinase ERK1/2 deactivation. Oncotarget 8(16):27339-27352.

Antonio PD, Lasalvia M, Perna G, Capozzi V (2012). Scale-independent roughness value of cell membranes studied by means of AFM technique. Biochimica et Biophysica Acta 1818(12):3141-3148.
Cai X, Xin X, Cai J, Chen Q, Wu S, Huang F (2010). Connection between biomechanics and cytoskeleton structure of lymphocyte and Jurkat cells: An AFM study. Micron 41(3):257-262.
Canetta E, Riches A, Borger E, Herrington S, Dholakia K, Adya AK (2014). Discrimination of bladder cancer cells from normal urothelial cells with high specificity and sensitivity: combined application of atomic force microscopy and modulated Raman spectroscopy. Acta biomaterialia 10(5):2043-2055.
Chhikara BS, Parang K (2010). Development of cytarabine prodrugs and delivery systems for leukemia treatment. Expert Opinion on Drug Delivery 7(12):1399-1414.
Chhikara BS, Parang K (2023). Global Cancer Statistics 2022: the trends projection análisis. Chemical Biology Letters 10(1):451.
Conter V, Rizzari C, Sala A, Chiesa R, Citterio M, Biondi A (2004). Acute Lymphoblastic Leukemia. Orphanet Encyclopedia 10(4):11-25.
Deng X, Xiong F, Li X, Xiang B, Li Z, Wu X, Xiong W (2018). Application of atomic force microscopy in cancer research. Journal of Nanobiotechnology 16(1):102.
Distelhorst C (2002). Recent insights into the mechanism of glucocorticosteroid-induced apoptosis. Cell Death & Differentiation 9(1): 6-19.
Dong S, Wang Q, Sun S, Liang Y, Jiang J, Liu L (2013). Atomic force microscopy of chronic lymphatic leukaemia cells activation induced by Staphylococcus aureus. Cell Biology International 37(4):380-386.
Francis LW, Lewis PD, Wright CJ, Conlan RS (2010). Atomic force microscopy comes of age. Biology of the Cell 102(2):133-143.
Greenstein S, Ghias K, Krett N, Rosen S (2002). Mechanisms of Glucocorticoid-mediated Apoptosis in Hematological Malignancies. Clinical Cancer Research 8:1681-1694.
Hiçsönmez G, Erdemli E, Tekelioglu M, Tuncer A, özbek N, Cetin M, Cotter T (1996). Morphologic Evidence of Apoptosis in Childhood Acute Myeloblastic Leukemia Treated with High-Dose Methylprednisolone. Leukemia & Lymphoma 22(1-2): 91-96.
Hiçsönmez G, Tuncer M, Toksoy H, Yenicesu I, Çetin M (1999). Differentiation of Leukemic Cells Induced by Short-Course High-Dose Methylprednisolone in Children with Different Subtypes of Acute Myeloblastic Leukemia. Leukemia & Lymphoma 33(5-6):573-580.
Hoffman EA, Brian L. Frey BL, Smith LM, Auble DT (2015). Formaldehyde Crosslinking: A Tool for the Study of Chromatin Complexes. The Journal of Biological Chemistry 290(44):26404-26411.
Horcas I, Fernández R, Gómez-Rodríguez J, Colchero J, Gómez-Herrero J, Baro A (2007). WSXM: A software for scanning probe microscopy and a tool for nanotechnology. Review of Scientific Instruments 78(1):13705.
Hu M, Wang J, Zhao H, Dong S, Cai J (2009). Nanostructure and nanomechanics analysis of lymphocyte using AFM: from resting, activated to apoptosis. Journal of biomechanics 42(10):1513-1519.
Huang X, He J, Liu M, Zhou C (2014). The influence of aminophylline on the nanostructure and nanomechanics of T lymphocytes: an AFM study. Nanoscale Research Letters 21 9(1):518.
Jembrek M J, Vlainić J, Čadež V, Šegota S (2018). Atomic force microscopy reveals new biophysical markers for monitoring subcellular changes in oxidative injury: Neuroprotective effects of quercetin at the nanoscale. PLOS ONE 13(10):1-22.
Khoirunnisa W, Puspitarini S, Rohmawati SA, Eltavia F, Rahayu RP, Utomo DH, Permatasari GW (2016). Molecular mechanism of formaldehyde and protein interaction in human cancer cell. Trends in Bioinformatics 9:30-34.
Kim K, Cho C, Park E, Jung M, Yoon K (2012). AFM-Detected Apoptotic Changes in Morphology and Biophysical Property Caused by Paclitaxel in Ishikawa and HeLa Cells. Plos One 7(1):1-9.
Kato M, Manabe A (2018). Treatment and biology of pediatric acute lymphoblastic leukemia. Pediatrics International 60(1):4-12.
Laane E, Tamm KP, Buentke E, Ito K, Kharaziha P, Oscarsson J, Corcoran M, Bjo¨ rklund A-C, Hultenby K, Lundin J, Heyman M, So¨ derha¨ll S, Mazur J, Porwit A, Pandolfi PP, Zhivotovsky B, Panaretakis T and Grande´r D (2009). Cell death induced by dexamethasone in lymphoid leukemia is mediated through initiation of autophagy. Cell Death and Differentiation 16:1018-1029.
Lambrou G, Papadimitriou L, Chrousos G, Vlahopoulos S (2012). Glucocorticoid and proteasome inhibitor impact on the leukemic lymphoblast: Multiple, diverse signals converging on a few key downstream regulators. Molecular and Cellular Endocrinology 351(2):142-151.
Larios-Farak TC, Rendón-García H, Ornelas-Ceballos JR, Covarrubias-Espinoza G, Ríos-García CG, Morales-Peralta A (2016). Supervivencia de niños con Leucemia Linfoblástica Aguda de riesgo intermedio. Boletín clínico del Hospital Infantil del Estado de Sonora 33(1):19-25.
Lastella M, Lasalvia M, Perna G, Biagi PF, Capozzi V (2007). Atomic force microscopy study on human keratinocytes treated with HgCl2. Journal of Physics: Conference Series 61(1):920.
Li M, Xi N, Wang Y, Liu L (2021). Atomic force microscopy for revealing micro/nanoscale mechanics in tumor metastasis: from single cells to microenvironmental cues. Acta Pharmacologica Sinica 42:323-339.
Liu J, Qu Y, Wang G, Wang X, Zhang W, Li J, Jiang J (2018). Study of morphological and mechanical features of multinuclear and mononuclear SW480 cells by atomic force microscopy. Microscopy research and technique 81(1):3-12.
Mayayo-Peralta I, Zwart W, Prekovic S (2021). Duality of glucocorticoid action in cancer: tumor-suppressor or oncogene?. Endocrine-Related Cancer 28:157-171.
Mayer LD, Tardi P, Louie AC (2019). CPX-351: A nanoscale liposomal co-formulation of daunorubicin and cytarabine with unique biodistribution and tumor cell uptake properties. International Journal of Nanomedicine 14: 3819-3830.
McNeer J, Nachman J (2010). The optimal use of steroids in pediatric acute lymphoblastic leukemia: no easy answers. British Journal of Hematology 149(5):638-652.
Mendoza-Santiago A, Becerra E, Garay E, Bah M, Berumen-Segura L, Escobar-Cabrera J, Hernández-Pérez A, García-Alcocer G (2019). Glutamic Acid Increased Methotrexate Polyglutamation and Cytotoxicity in a CCRF-SB Acute Lymphoblastic Leukemia Cell Line. Medicina 55:758.
Nečas D, Klapetek P (2012). Gwyddion: an open-source software for SPM data analysis. Open Physics 10(1):181-188.
Özbek N, Erdemli E, Hiçsönmez G, Okur H, Tekelioğlu M (1999). Effects of Methylprednisolone on Human Myeloid Leukemic Cells In Vitro. American Journal of Hematology 60:255-259.
Padmakumar D, Chandraprabha VR, Gopinath P, Devi ARTV, Anitha GR J, Sreelata MM, Padmakumar A, Sreedharan H (2021). A concise review on the molecular genetics of acute myeloid leukemia. Leukemia Research 111:106727.
Pan Y, Liu XY, Liu JQ, Liu Q, Yang Y, Yang JL, Wang YZ (2016). Necroptosis: a new link between cell death and inflammation. Neuroimmunology Neuroinflammation 3:156-160.
Patel AN, Kranz C (2018). Multi-functional Atomic Force Microscopy Imaging. Annual Review of Analytical Chemistry 11:329-350.
Pillet F, Chopinet L, Formosa C, Dague É (2013). Atomic Force Microscopy and pharmacology: From microbiology to cancerology. Biochimica et Biophysica Acta 1840:1028-1050.
Rendón-García H, Tamayo-Pedraza G, Covarrubias-Espinoza G (2017). Ventana de esteroide en niños con Leucemia Linfoblástica Aguda evaluada por factores pronósticos. Boletín Clínico del Hospital Infantil del Estado de Sonora 34(2):82-89.
Szende B, Tyihák E (2010). Effect of formaldehyde on cell proliferation and death. Cell Biology International 34(12):1273-1282.
Smith L, Cidlowski J (2010). Glucocorticoid-Induced Apoptosis of Healthy and Malignant Lymphocytes. Neuroendocrinology – Pathological Situations and Diseases 148:1-30.
Schwartzman RA, Cidlowski JA (1994). Glucocorticoid-induced apoptosis of lymphoid cells. International Archives of Allergy and Immunology 105(4):347-354.
Terwilliger T, Abdul-Hay M (2017). Acute lymphoblastic leukemia: a comprehensive review and 2017 update. Blood Cancer Journal 7:e577.
Thavarajah R, Mudimbaimannar VK, Elizabeth J, Rao UK, Ranganathan K (2012). Chemical and physical basics of routine formaldehyde fixation. Oral Maxillofacial Pathology 16(3):400-405.
Timmermans S, Souffriau J, Libert C (2019). A General Introduction to

Glucocorticoid Biology. Fronteirs in Immunolgy Section Inflammation 10:1545.
Tissing W, Meijerink J, den Boer M, Pieters R (2003). Molecular determinants of glucocorticoid sensitivity and resistance in acute lymphoblastic leukemia. Leukemia 17(1):17-25.
Velentza L, Zaman F, S¨avendahl L (2021). Bone health in glucocorticoid-treated childhood acute lymphoblastic leukemia. Critical Reviews in Oncology/Hematology 168:103492.
Walsh CM, Edinger AL (2010). The complex interplay between autophagy, apoptosis, and necrotic signals promotes T-cell homeostasis Immunology Review 236: 95-109.
Wang J, Wan Z, Liu W, Li L, Ren L, Wang X, Zhang Z (2009). Atomic force microscope study of tumor cell membranes following treatment with anti-cancer drugs. Biosensors and Bioelectronics 25(4):721-727.
Wang Y, Xu C, Jiang N, Zheng L, Zeng J, Qiu C, Xie S (2016). Quantitative analysis of the cell-surface roughness and viscoelasticity for breast cancer cells discrimination using atomic force microscopy. Scanning 38:558-563**.**
Wu Y, Lu H, Cai J, He X, Hu, Y, Zhao H, Wang X (2009). Membrane Surface Nanostructures and Adhesion Property of T Lymphocytes Exploited by AFM. Nanoscale Research Letters 4(8):942-947.
Yetgin S, Özsoylu S (2007). Comparison of Megadose Methylprednisolone Versus Conventional Dose Prednisolone in Hematologic Disorders. Journal of Pediatric Hematology/ Oncology 29(4):253-259.
Zhang Z, Dong L, Jia A, Chen X, Yang Q, Wang Y, Wang Y, Liu R, Cao Y, He Y, Bi Y, Liu G (2020). Glucocorticoids Promote the Onset of Acute Experimental Colitis and Cancer by Upregulating Mtor Signaling in Intestinal Epithelial Cells. Cancers 12:945.
Zhao S, Li Y, Wang Y, Ma Z, Huang X (2019). Quantitative study on coal and shale pore structure and surface roughness based on atomic force microscopy and image processing. Fuel 244:78-90.
Zhao W, Li Y, Yao C, Zhang G, Zhao KY, Chen W, Ru P, Pan X, Tu H, Jones D (2020). Detection of Pathogenic Isoforms of IKZF1 in Leukemic Cell Lines and Acute Lymphoblastic Leukemia Samples: Identification of a Novel truncated IKZF1 Transcript in SUP-B15, 2020. Cancers 12(11):3161.